

Cross-correlation Tomography: Measuring Dark Energy Evolution with Weak Lensing

Bhuvnesh Jain¹ and Andy Taylor²

¹ Department of Physics and Astronomy, University of Pennsylvania, Philadelphia, PA 19104, U.S.A.

² Institute for Astronomy, Royal Observatory, Blackford Hill, Edinburgh, EH9 3HJ, U. K.

A cross-correlation technique of lensing tomography is presented to measure the evolution of dark energy in the universe. The variation of the weak lensing shear with redshift around massive foreground objects like bright galaxies and clusters depends solely on the angular diameter distances. Use of the massive foreground halos allow us to compare relatively high, linear shear amplitudes in the same part of the sky, thus largely eliminating the dominant source of systematic error in cosmological weak lensing measurements. The statistic we use does not rely on knowledge of the foreground mass distribution and is only shot-noise limited. We estimate the constraints that deep lensing surveys with photometric redshifts can provide on the dark energy density Ω_{de} , the equation of state parameter w and its redshift derivative w' . The marginalized accuracies on w and w' are: $\sigma(w) \simeq 0.01 f_{\text{sky}}^{-1/2}$ and $\sigma(w') \simeq 0.03 f_{\text{sky}}^{-1/2}$, where f_{sky} is the fraction of sky covered by the survey and $\sigma(\Omega_{\text{de}}) = 0.03$ is assumed in the marginalization. The strength of the method lies in its constraints on the evolution of dark energy: a deep lensing survey that covers 1/10 of the sky would constrain w' to 10% accuracy. Combining our cross-correlation method with standard lensing tomography, which has orthogonal degeneracies, will allow measurement of the dark energy parameters with significantly better accuracy.

I. INTRODUCTION

Gravitational lensing provides us with the most direct method for probing the distribution of matter in the universe [1]. Lensing leads to a shear distortion of background galaxy images, or a change in the surface number density of background galaxies due to magnification. The measurement of the mass distribution in clusters of galaxies using the lensing shear [2, 3] and magnification [4, 5, 6, 7] are now well established techniques. On larger scales detections of the cosmic shear signal [8] show that the cosmological matter distribution can also be probed this way.

The variation of the lensing signal for background galaxies at different redshifts probes the projected lensing mass with different redshift weights in a way that depends on cosmology [9, 10, 11, 12]. Hu [12, 13, 14] has developed techniques for using the shear power spectrum for background galaxies with photometric redshift information to constrain cosmological parameters, in particular the nature and evolution of dark energy. His and other recent studies [15, 16, 17, 18, 19, 20] have forecast the accuracy with which these parameters can be obtained from future weak lensing surveys, while [21, 22] have developed methods to use tomography for 3-D mass reconstruction. Observationally weak lensing tomography has been applied to a galaxy cluster [23], but further progress awaits multi-color imaging surveys that can obtain photometric redshifts of background galaxies.

The lensing shear (or magnification bias) can be used to cross-correlate large foreground galaxies (associated with the lensing mass) with background galaxies which are lensed. In this paper we will use such cross-correlations as an alternative way of doing lensing tomography. We use a particularly simple cross-correlation statistic: the average tangential shear around massive foreground halos associated with galaxy groups

and galaxy clusters. We show that cross-correlation tomography measures ratios of angular diameter distances over a range of redshifts. The distances are given by integrals of the expansion rate, which in turn depends on the equation of state of the dark energy. Thus it can be used to constrain the evolution of dark energy. We estimate the accuracy with which dark energy parameters can be measured from future lensing surveys.

II. FORMALISM

We work with the metric

$$ds^2 = a^2 [-(1+2\phi)d\tau^2 + (1-2\phi)(d\chi^2 + r^2 d\Omega^2)], \quad (1)$$

where we have used the comoving coordinate χ and $a(\tau) = (1+z)^{-1}$ is the scale factor as a function of conformal time τ . We adopt units such that $c = 1$. The comoving angular diameter distance $r(\chi)$ depends on the curvature: we assume a spatially flat universe so that $r(\chi) = \chi$. The density parameter Ω has contributions from mass density Ω_m or dark energy density Ω_{de} , so that $\Omega = \Omega_m + \Omega_{\text{de}}$. The dark energy has equation of state $p = w\rho$, with $w = -1$ corresponding to a cosmological constant. The Hubble parameter $H(a)$ is given by

$$H(a) = H_0 \left[\Omega_m a^{-3} + \Omega_{\text{de}} e^{-3 \int_1^a d\ln a' (1+w(a'))} \right]^{\frac{1}{2}}, \quad (2)$$

where H_0 is the Hubble parameter today. The comoving distance $\chi(a)$ is

$$\chi(a) = \int_1^a \frac{da'}{a'^2 H(a')}, \quad (3)$$

The lensing convergence is given by the weighted projection of the mass density

$$\kappa(\hat{\phi}) = \frac{3}{2}\Omega_m \int_0^{\chi_0} d\chi g(\chi) \frac{\delta(r\hat{\phi}, \chi)}{a} , \quad (4)$$

where the radial weight function $g_b(\chi)$ can be expressed in terms of $r(\chi)$ and the normalized distribution of background galaxies $W_b(\chi)$

$$g_b(\chi) = r(\chi) \int_{\chi}^{\chi_0} \frac{r(\chi' - \chi)}{r(\chi')} W_b(\chi') d\chi' , \quad (5)$$

where χ_0 is the distance to the horizon. For a delta-function distribution of background galaxies at χ_b , this reduces to $g_b(\chi) = r(\chi)r(\chi_b - \chi)/r(\chi_b)$.

We consider the lensing induced cross-correlation between massive foreground halos, which are traced by galaxies, and the tangential shear with respect to the halo center (denoted γ in this paper): $\omega_{\times}(\theta) \equiv \langle \delta n_f(\hat{\phi}) \gamma(\hat{\phi}') \rangle$ where $n_f(\hat{\phi})$ is the number density of foreground galaxies with mean redshift $\langle z_f \rangle$, observed in the direction $\hat{\phi}$ in the sky and $\delta n_f(\hat{\phi}) \equiv (n_f(\hat{\phi}) - \bar{n}_f)/\bar{n}_f$. The angle between directions $\hat{\phi}$ and $\hat{\phi}'$ is θ . The cross-correlation is given by [24],[25]:

$$\begin{aligned} \omega_{\times}(\theta) = & 6\pi^2 \Omega_m \int_0^{\chi_H} d\chi W_f(\chi) \frac{g_b(\chi)}{a(\chi)} \\ & \times \int_0^{\infty} dk k P_{\text{hm}}(\chi, k) J_{\mu} [kr(\chi)\theta] , \end{aligned} \quad (6)$$

where $P_{\text{hm}}(\chi, k)$ is the halo-mass cross-power spectrum, and W_f is the foreground halo redshift distribution. The Bessel function J_{μ} has subscript $\mu = 2$ for the tangential shear and $\mu = 0$ for the convergence (from the relation $\gamma(\theta) = -1/2 d\bar{\kappa}(\theta)/d\ln\theta$, [25]). The measurement of the mean tangential shear around foreground galaxies is called galaxy-galaxy lensing. We will consider a generalization of this to massive halos that span galaxy groups and clusters.

If the foreground sample has a narrow redshift distribution centered at $\chi = \chi_f$, then we can take W_f to be a Dirac-delta function and evaluate the integral over χ . All terms except $g_b(\chi_f)$ are then functions of χ_f , the redshift of the lensing mass. The coupling of the foreground and background distributions is contained solely in $g_b(\chi_f)$. Hence if we take the ratio of the cross-correlation for two background populations with mean redshifts z_1 and z_2 , we get

$$\frac{w_1(\theta)}{w_2(\theta)} = \frac{g_1(\chi_f)}{g_2(\chi_f)} , \quad (7)$$

where w_1, g_1 denote the values of the functions for the background population with mean redshift z_1 . In the limit that the background galaxies also have a delta-function distribution, this is simply a ratio of distances

$$\frac{w_1(\theta)}{w_2(\theta)} = \frac{r(\chi_1 - \chi_f)/r(\chi_1)}{r(\chi_2 - \chi_f)/r(\chi_2)} \quad (8)$$

The above equations show that the change in the cross-correlation with background redshift does not depend on the galaxy-mass power spectrum, nor on θ . We can simply use measurements over a range of θ to estimate the distance ratio of equation (8) for each pair of foreground-background redshifts. The distance ratio in turn depends on the cosmological parameters Ω_{de} , w , and its evolution w' . We evaluate next how the cross-correlation defined above can be used to constrain the dark energy parameters. This approach is complementary to standard lensing tomography, where the variation of power spectrum of the shear with background redshifts is used to measure an integral of distance and growth factors over redshift. With the cross-correlations, there is no dependence on growth factor, but a precise dependence on distances (since they are not integrated over redshift).

III. RESULTS

A. Signal-to-noise estimate

A simple way to estimate the signal-to-noise for the cross-correlation approach is to regard the foreground galaxies as providing a template for the shear fields of the background galaxies (G. Bernstein, private communication). For a perfect template (i.e. for high density of foreground galaxies and no biasing), the errors are solely due to the finite intrinsic ellipticities of background galaxies. Thus the fractional error in our measurement of the background shears is simply

$$\frac{\delta\gamma}{\gamma} \sim \frac{\sigma_{\epsilon}}{\sqrt{N_{\text{total}}} \langle \gamma \rangle_{\text{rms}}} . \quad (9)$$

The total number of background galaxies is $N_{\text{total}} = n_g A = n_g f_{\text{sky}} A_{\text{sky}}$, where A is the survey area, the lensing induced rms shear $\langle \gamma \rangle_{\text{rms}} \simeq 0.04$ [9], and the intrinsic ellipticity dispersion $\sigma_{\epsilon} = 0.3$. This gives

$$\frac{\delta\gamma}{\gamma} \sim 0.2 \times 10^{-3} \left(\frac{100}{n_g} \right)^{1/2} \left(\frac{0.1}{f_{\text{sky}}} \right)^{1/2} , \quad (10)$$

where the number density n_g has units per square arcminute. Thus for the fiducial parameters $f_{\text{sky}} = 0.1$ and $n_g = 100$, one can expect to measure the background shear to 0.1% accuracy at about 5σ . We find that such a signal corresponds to changes in w of a few percent; hence this is the approximate sensitivity we expect in the absence of systematic errors.

B. Models

To construct a simple and observationally robust cross-correlation statistic, we restrict the foreground sample to galaxy clusters and large galaxy groups. With deep imaging surveys, most of these massive objects are expected to

be identified out to $z \sim 1$. We use the tangential component of the shear for two background samples at different redshifts, inside apertures of size $\theta_{\text{ap}} \sim 3'$, as our estimator of the distance ratio of equation (7). The signal from all massive halos in a given redshift bin will be stacked for each background sample. The tangential shear around a foreground halo is $\langle \gamma(\theta) \rangle = (\bar{\Sigma}(\theta) - \Sigma(\theta)) / \Sigma_{\text{crit}}$ where Σ_{crit} is the geometrical factor that depends on angular diameter distances. To compute the average shear around halos within a mass range, one replaces the projected mass density Σ by the projection of the halo-mass correlation function, so that the above equation is equivalent to equation (6) in the limit of thin redshift distributions. We will assume that the massive foreground halos at $z < 1$ have spectroscopic or accurate photometric redshifts, since they generally contain at least one bright galaxy. Each background galaxy sample is described by a redshift distribution determined using photometric redshifts (which can have relatively large statistical errors).

The average tangential shear around foreground galaxies and clusters has proven easier to measure than shear-shear correlations since it is linear in the shear and has a distinct signal that can be distinguished from systematic contributions (for a wide field survey it is unlikely for a systematic to produce an averaged tangential shear around foreground galaxies). Moreover, in comparing the signal for two background populations, it is a great advantage that the shear amplitudes are compared for the same set of apertures on the sky: the relative amplitudes are insensitive to spatial variations of the point spread function, which are the dominant systematic for shear-shear correlations.

To compute the accuracy with which parameters can be measured, we need to compute the signal and the noise. The signal is given by equation (6) in which the halo-mass cross-correlation can be accurately computed using the halo model of large-scale structure (see [26] for a review). The model specifies $n(m, z)$, the comoving number density of halos with mass m , the bias parameter of halos, and the density profile of a halo for given mass and redshift. Details of the model ingredients relevant to this study are given in [27, 28].

The two key quantities for each redshift bin is the number density of halos and the mean shear for each halos mass. We choose the mass range $4 \times 10^{13} < m / M_{\odot} < 10^{15}$ and aperture size $\theta_{\text{ap}} = 2' - 5'$ corresponding roughly to the virial radii of halos over the redshift range used. We also set a constant inner aperture $\theta = 0.1'$ to exclude the strong lensing regime and the luminous parts of the lensing halos. With foreground redshift slices of width $\Delta z = 0.1$, the halos in each slice cover about 1/10 the survey area. Thus using all the foreground slices over $0 < z_f < 1$, close to the entire survey area is covered.

We take the background redshift distribution to be given by $dN/dz \sim z^a \exp[-(z/z_0)^b]$, with $a = 2$ and $b = 1.5$ and $z_0 = 1$ giving a mean redshift of 1.5. We normalize it to give a total number of density $n_g = 100$ per square arcminute. It is split into two background

samples, between z_f and $z = 3.0$, with about half the galaxies in each sample. The halo model is used to obtain the mean shear for each lens-source redshift distribution by summing the contributions of halos over the chosen mass range. While we have used the halo model to compute the expected signal-to-noise, the inferred parameter values do not rely on knowing the masses or any properties of the halos.

C. Dark energy parameters

We perform a χ^2 minimization over the mean shear amplitudes at the two background distributions for each foreground slice to fit for the dark energy parameters. The time dependence of w is parameterized as $w = w_0 + w_a(1 - a)$ [30]. For comparison with other work we will compare w_a to w' defined by $w = w_0 + w'z$. Since the w' parameterization is unsuitable for the large redshift range we use, any comparison with it can be made only for a choice of redshift. For example, at $z = 1$, which is well probed by our method and is of interest in discriminating dark energy models [30], $w_a = 2w'$. For foreground slices labeled by index l and two background samples by 1 and 2, the χ^2 is given by

$$\chi^2 = \sum_l \left[1 - \frac{R^0(z_l, z_1, z_2)}{R(z_l, z_1, z_2)} \right]^2 U_l, \quad (11)$$

where R is the distance ratio of equation (7) for given values of Ω_{de} , w and w_a , and R^0 is the fiducial model with $\Omega_{\text{de}} = 0.7, w = -1, w_a = 0$. The weights U_l are given by

$$U_l^{-1} = \frac{\sigma_{\epsilon}^2}{2n_1 f_l A \langle \gamma \rangle_{l1}^2} + \frac{\sigma_{\epsilon}^2}{2n_2 f_l A \langle \gamma \rangle_{l2}^2}, \quad (12)$$

where f_l is the fraction of the survey area A covered by halo apertures in the l -th lens slice. The factor of 2 in the denominator arises because we are using only one component of the measured ellipticity whereas σ_{ϵ}^2 denotes the sum of the variances of both components.

The results are shown in Figures 1 and 2. Figure 1 shows the constraints in the $\Omega_{\text{de}} - w$ plane. The ellipses show the 68% confidence region given by $\Delta\chi^2 = 2.3$. The elongated inner contour is for fixed $w_a = 0$. The two outer contours marginalize over w_a assuming external constraints on Ω_{de} from the CMB and other probes, corresponding to $\sigma(\Omega_{\text{de}}) = 0.01, 0.03$.

Figure 2 shows the constraints in the $w - w_a$ plane if Ω_{de} is fixed, or marginalized over with $\sigma(\Omega_{\text{de}}) = 0.01, 0.03$. The corresponding accuracy on w and w' can be scaled as $f_{\text{sky}}^{-1/2}$. For the case with $\sigma(\Omega_{\text{de}}) = 0.03$, we obtain $\sigma(w) \simeq 0.01 f_{\text{sky}}^{-1/2}$ and $\sigma(w_a) \simeq 0.06 f_{\text{sky}}^{-1/2}$ (at $z = 1$ this is equivalent to $\sigma(w') \simeq 0.03 f_{\text{sky}}^{-1/2}$). Note that the value of σ on a parameter is given by projecting the $\Delta\chi^2 = 1$ contour on the parameter axis, which is

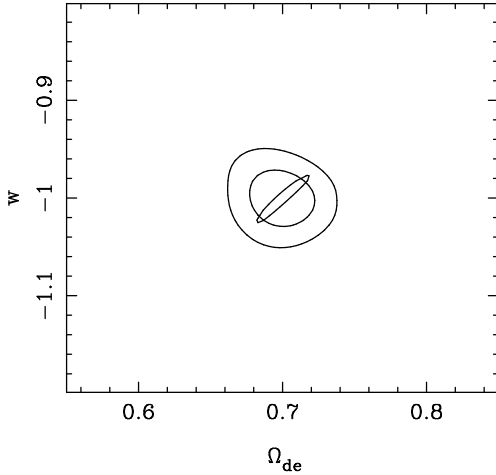


FIG. 1: Contours in the $\Omega_{\text{de}} - w$ plane for the fiducial lensing survey with $f_{\text{sky}} = 0.1$. The inner contour assumes no evolution of dark energy, $w_a = 0$, while the two outer contours marginalize over w_a , with external constraints on Ω_{de} corresponding to $\sigma(\Omega_{\text{de}}) = 0.01, 0.03$ (see text). The 68% confidence interval is shown in each of the contours.

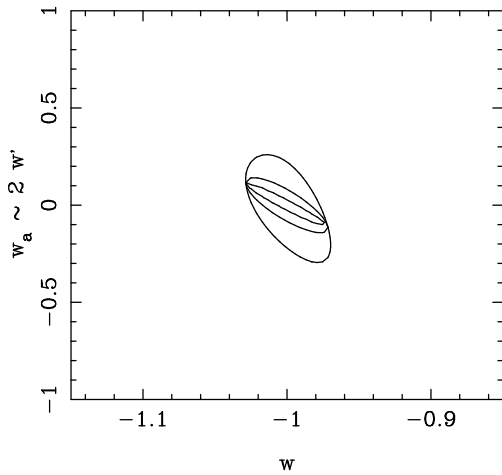


FIG. 2: Contours in the $w - w'$ plane for the fiducial lensing survey with $f_{\text{sky}} = 0.1$, as in Figure 1. The inner contour assumes $\Omega_{\text{de}} = 0.7$, while the outer two contours marginalize over Ω_{de} as in Figure 1. Note that the parameter $w_a = 2 w'$ at $z = 1$ (see discussion in the text).

IV. DISCUSSION

smaller than the projection of the inner contour in Figure 2 with $\Delta\chi^2 = 2.3$. The scaling with f_{sky} in the parameter errors comes from the number of background galaxies (not sample variance), hence for given f_{sky} varying the depth of the survey scales the errors roughly as $n_g^{-1/2}$. The results we have shown are for the fiducial redshift $z = 0$. A different choice of the fiducial redshift changes the relative accuracy on w and w_a somewhat, because the degeneracy direction in the three parameters changes. A detailed exploration of different models of $w(a)$ with finer bins in the background redshift distribution would be of interest.

The parameter constraints obtained above are consistent with the crude signal-to-noise estimate made above in equation (10). This can be seen by using representative numbers for the halos used in the cross correlation. For $m = 10^{14} M_\odot$, the number density $n(m) \sim 0.01/\text{arcmin}^2$ per \ln interval in m integrated out to $z = 1$, while the mean shear inside $\theta_{\text{ap}} = 3'$ is $\langle \gamma \rangle \simeq 5\%$ for $z_f = 0.3$ and $z_b = 1$ [28]. Thus using halos with a mass range of one decade centered on $m = 10^{14} M_\odot$ gives close to full sky coverage. For relevant scales, the shear profile around the halo center is close to the isothermal form: $\gamma \propto 1/\theta$. The signal-to-noise is then constant per $\log \theta$ since the noise variance scales as the area ($\propto \theta^2$). Thus the rather simple scheme of stacking all halos, and averaging over the mean shear inside apertures, gives a good estimate of the signal. The noise per unit area is $\sigma_\epsilon / \sqrt{2n_g}$. Using the numbers given above for $\langle \gamma \rangle$ and the noise gives a signal-to-noise estimate in agreement with equation (10) as well as the results shown in Figures 1 and 2.

We have presented a method of lensing tomography that uses foreground halos associated with the lensing mass to measure angular diameter distances over a range of redshifts, $0 \lesssim z \lesssim 3$. It offers an observationally robust probe of dark energy and its evolution over this redshift range. The accuracy achievable with a lensing survey that covers 1/10 of the sky (with parameters close to that of the survey proposed with the LSST telescope) is better than 5% in w and 10% in its evolution parameterized as w' . This accuracy on the evolution parameter of dark energy is potentially one of the most promising for proposed surveys in the coming decade. It is complementary with constraints from Type 1a supernovae in that the redshift coverage is broader while the distance factors probed are similar [20]. Combining cross-correlation tomography with the standard shear power spectrum tomography improves the constraints significantly, since the contour ellipses are oriented differently [14] – this is especially appealing because the two techniques use the data in different regimes, the linear and strongly nonlinear regime. Further it would allow the constraints on the dark matter, such as on neutrino mass, from shear power spectrum tomography to be improved by providing independent information on the geometry.

We believe that the most attractive feature of cross-correlation tomography is its observational feasibility. The main practical advantages are: (i) large shear values ($\sim 1 - 10\%$) around massive halos are used, and (ii) linear shear amplitudes are compared in the *same* apertures on the sky. The statistic is thus largely insensitive to the primary limiting systematic error in weak lensing surveys:

the variation of the point spread function over the field view (to first order the psf variation averages to zero for a linear statistic). The imaging requirements are far less stringent than for other cosmological applications of lensing, such as standard tomography, which rely on the measurement of quadratic shear correlations at large angles. The ongoing CFH Legacy survey should allow for testing of the method and parameter constraints that can be checked with limits from the CMB. The limiting systematic error for most surveys is likely come from the photometric redshifts of the background galaxies. While large statistical errors do not affect the parameter constraints significantly, systematic errors could bias the inferred distance ratios. Calibrating a fair sub-sample of the photometric redshifts with spectroscopic redshifts, and testing for effects such as possible correlations between measured ellipticities and the sizes or surface brightness of galaxies, should allow us to safeguard against such biases.

We have assumed in this study that the intrinsic ellipticities of background galaxies dominate the statistical errors. Other sources of errors are projection effects due to matter at different redshifts from the foreground halo and intrinsic correlations in the ellipticities of background galaxies. Our choice of averaging the tangential shears around halos should cause these errors to average to zero, but a careful study is needed to quantify the contribution to the statistical error. A possible bias can be introduced if the foreground redshifts have large errors and the halo selection, based on visible galaxies, is perversely correlated with dark energy evolution. Statistical accuracy in the foreground redshifts of better than 0.1 in z should

rule out such a bias due to cosmological evolution, but again a more detailed study is needed.

Our implementation of halo-shear cross-correlations is not optimal in that we have used only a fraction of the measured shapes for each lens slice, and only two bins of the background galaxies (motivated in part by the finding that this provides most of the information in shear power spectrum tomography [12]). The parameter accuracy can therefore be improved with an optimal scheme in which we use finer binning or the actual redshifts (or photometric redshift probability distributions) of foreground and background galaxies rather than binning them. It will also be of interest to study different models of $w(z)$ rather than the monotonic parameterization used here, or to obtain model independent constraints on the expansion history directly [29, 30]. A joint analysis with shear-shear correlations is needed to quantify the improved precision one can expect. We have restricted ourselves to the weak lensing shear; additional information can be obtained by using the strong lensing signal expected in some fraction of the galaxy and cluster halos (for related studies with lensing arcs from galaxy clusters, see [31, 32, 33]) and using the magnification signal.

Acknowledgments: We thank G. Bernstein for many insightful conversations. We thank E. Bertschinger, A. Heavens, W. Hu, M. Jarvis, E. Linder, U. Pen, R. Sheth and M. Takada for helpful discussions. BJ is supported by NASA grant NAG5-10923 and a Keck foundation grant. ANT thanks the PPARC for an Advanced Research Fellowship and the University of Pennsylvania for its hospitality while this work was in development.

[1] Y. Mellier, *Ann. Rev. Astron. Astrophys.*, **37**, 127 (1999);
 M. Bartelmann, P. Schneider, *Phys. Rept.*, **340**, 291 (2001);

[2] J.A. Tyson, R.A. Wenk, F. Valdes, *Astrophys. J.*, **349**, L1 (1990).

[3] N. Kaiser, G. Squires, *Astrophys. J.*, **404**, 441 (1993)

[4] J.A. Tyson, *Astron. J.*, **96**, 1 (1998)

[5] T. Broadhurst, A. Taylor, J. Peacock, *Astrophys. J.*, **438**, 49 (1995)

[6] B. Fort, Y. Mellier, M. Dantel-Fort, *A&A*, **321**, 353 (1997)

[7] A. N. Taylor, et al., *Astrophys. J.*, **501**, 539 (1998).

[8] D. Bacon, A. Refregier, R. Ellis, *Mon. Not. Roy. Astr. Soc.*, **318**, 625 (2000); N. Kaiser, G. Wilson, G.A. Luppino, *Astrophys. J. Lett.*, submitted, astro-ph/0003338 (2000); L. van Waerbeke, et al. *Astron. Astrophys.*, **358**, 30 (2000); D.M. Wittman, J.A. Tyson, D. Kirkman, I. Dell'Antonio, G. Bernstein, *Nature*, **405**, 143 (2000).

[9] B. Jain, U. Seljak, *Astrophys. J.*, **484**, 560 (1997).

[10] N. Kaiser, *Astrophys. J.*, **498**, 26 (1998).

[11] U. Seljak, *Astrophys. J.*, **506**, 64 (1998).

[12] W. Hu, *Astrophys. J. Lett.*, **522**, 21 (1999).

[13] W. Hu, *Phys. Rev. D* **65**, 023003 (2002).

[14] W. Hu, *Phys. Rev. D* **66**, 083515 (2002)

[15] D. Huterer, *Phys. Rev. D*, **65**, 063001 (2002).

[16] K. N. Abazajian, S. Dodelson, arXiv:astro-ph/0212216.

[17] A. Heavens, arXiv:astro-ph/0304151.

[18] A. Refregier *et al.*, arXiv:astro-ph/0304419.

[19] L. Knox, arXiv:astro-ph/0304370.

[20] E. V. Linder and A. Jenkins, arXiv:astro-ph/0305286.

[21] A.N. Taylor, *Phys. Rev. Lett.*, submitted, astro-ph/0111605 (2001).

[22] W. Hu, C.R. Keeton, *Phys. Rev. D*, in press, astro-ph/0205412 (2002).

[23] D. Wittman, J.A. Tyson, V.E. Margoniner, J.G. Cohen, I.P. Dell'Antonio, *Astrophys. J.*, **557**, 89 (2001).

[24] R. Moessner and B. Jain, *Mon. Not. Roy. Astr. Soc.*, **294**, L18 (1998).

[25] J. Guzik and U. Seljak, *Mon. Not. Roy. Astr. Soc.*, **335**, 311 (2002).

[26] A. Cooray and R. Sheth, *Phys. Rept.* **372**, 1 (2002).

[27] B. Jain, R. Scranton and R. K. Sheth, arXiv:astro-ph/0304203.

[28] M. Takada and B. Jain, arXiv:astro-ph/0304034.

[29] M. Tegmark, *Phys. Rev. D*, submitted, astro-ph/0101345 (2001).

[30] E. V. Linder, arXiv:astro-ph/0210217.

[31] R. Link and M. J. Pierce, *Astrophys. J. Lett.*, **502**, 63 (1998).

[32] G. Golse, J. P. Kneib and G. Soucail, arXiv:astro-ph/0205357.

[33] M. Sereno, *Astron. Astrophys.* **393**, 757 (2002).